

Study on high-temperature resistance, salt/calcium resistance of environment-friendly colloidal gas aphon drilling fluid

Wenxi Zhu ^{a,*}, Bingjie Wang ^{a,b}, Xiuhua Zheng ^c

a. School of Civil Engineering and Architecture, Henan University, Henan, P. R. China.

b. Engineering Research Center of Geothermal Resources Development Technology and Equipment, Ministry of Education, Jilin University, Changchun, China.

c. School of Engineering and Technology, China University of Geosciences (Beijing), Beijing, P.R. China.

* Corresponding author: zhuwenxidida@163.com (W. Zhu)

Received 18 September 2023; Received in revised form 13 November 2023; Accepted 20 January 2024

Keywords

CGA drilling fluid;
Environmentally friendly;
Underbalanced drilling;
High-temperature
resistance;
 $\text{Ca}^{2+}/\text{Na}^+$ contamination
tolerance.

Abstract

The Colloidal Gas Aphron (CGA) drilling fluid successfully solved the problems of lost circulation and reservoir damage that are faced by drilling in depleted oil/gas reservoirs and low-pressure areas. However, the lack of high-temperature resistance, salt/calcium resistance are the key problems that restrict its application in complex formations. This study provides an environmentally friendly and non-toxic CGA formula based on self-developed reagents. Microscopic tests showed that stable aphrons were successfully generated in 36% NaCl-CGA or 7.5% CaCl₂-CGA aged at 150°C, with stabilization of >2 h. The Herschel-Bulkley model accurately describes the rheological behavior of CGA fluids containing NaCl/CaCl₂. The addition of NaCl increases CGA fluid viscosity, while CaCl₂ is the opposite. However, CGA fluid maintains appropriate rheological parameters and shear thinning behavior, which means good cutting carrying capacity. With the addition of NaCl/CaCl₂, CGA has low filtration volumes, which meets American Petroleum Institute (API) requirements. NaCl/CaCl₂ reduces the lubrication coefficient and increases the adhesion of the mud cake. Moreover, the anti-cuttings pollution ability of 150°C aged CGA can reach 10%. CGA, 36% NaCl-CGA, and 7.5% CaCl₂-CGA all have low linear expansion rates (<28%) and high rolling recovery rates (>84%). Therefore, the CGA system has good inhibitory performance and is compatible with easily hydrated formations.

1. Introduction

Recently, a near-balanced drilling technology, the Colloidal Gas Aphron (CGA) drilling fluid has been successfully applied in drilling depleted oil/gas reservoirs and other under-pressure areas [1]. It is a near/under-balanced technology which is composed of independent rigid micro-foams with bubble size ~100 μm , and has the following significant advantages: (a) As shown in Figure 1, the aphrons are composed of one core and three films. The unique structure makes it have high stability and strong pressure-bearing capacity, which is nearly 10 times that of ordinary foam [2]. Through cyclic pressure/relief experiments and

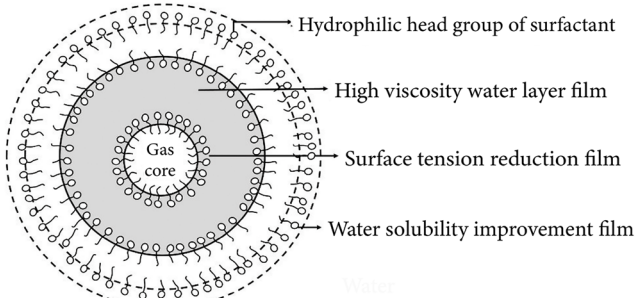
pressure sealing experiments, Jianyu et al. [3] confirmed that under a pressure of 20 MPa, CGA has compressibility and recovery properties, and can effectively seal sandstone formations of 40-60 mesh. Pasdar et al. [4] monitored the behavior of CGA under high pressure using a high-pressure microscope and studied the single bubble behavior and bubble size distribution of CGA. Observations indicate that CGA survived at pressures as high as 13.8 MPa may support the idea for field applications of CGA as drilling fluids. Zhu and Zheng [5] combined microscopy and HTHP filtration experiments to further demonstrate the sealing performance

To cite this article:

W. Zhu, B. Wang, X. Zheng "Study on high-temperature resistance, salt/calcium resistance of environment-friendly colloidal gas aphon drilling fluid", *Scientia Iranica* (2025) 32(9): 8225. <https://doi.org/10.24200/sci.2024.63113.8225>

Table 1. Application status of CGA drilling fluid in the field.

| Year | Main components | Drilling fluid properties | Field application |
|-----------|--|---|---|
| 2005 [47] | Foaming agent HYF and foam stabilizer CMC | $\rho: 0.75\sim0.96 \text{ g/cm}^3$; $\text{FL} < 10 \text{ mL}$; $YP/PV: 0.62\sim0.95$. | It effectively solves the problems of serious lost circulation in northeastern Sichuan. Compared with similar wells in adjacent areas, the drilling speed is increased by 3~7 times, the drilling time is shortened by 29.5 days, and the direct economic benefit is more than 1 million ¥. |
| 2016 [48] | Foaming agent LF-2 and foam stabilizer HMC-1, viscosity increasing agent HT-XC, fluid loss agent KH-931 and SMP-II | $\rho: 0.85\sim0.95 \text{ g/cm}^3$; $\text{FL} < 7.4 \text{ mL}$; Strong inhibitory and blocking ability; Temperature resistance: 150°C. | The system is used in 21 wells in the oilfields of Cicai, Shencai, and Shenleng, with a maximum well depth of 4005m and a maximum temperature of 141.5°C. Compared with adjacent wells, the ROP in the same layer is increased by 70% after the use of microbubble drilling fluid. |
| 2018 [49] | Foaming agent TSB and foam stabilizer HV-PAC | $\rho: 1.08 \text{ g/cm}^3$; $\text{FL} < 5 \text{ mL}$; Strong suspension carrying ability and inhibition; Salt resistance: 15%. | It is applied to the well section (2542-2837m) of the Kizivolda gas field in Kazakhstan. The system has a low density and stable wellbore, and there is no scratching or obstruction when drilling large sections of mudstone, gypsum, and gypsum mudstone. |
| 2021 [50] | Foaming agent LHPF-1 and BS-12, foam stabilizer XG | $\rho: 0.93\sim0.95 \text{ g/cm}^3$; The plugging rate and penetration recovery rate $>90\%$; Cuttings resistance: 7%. | It is applied to coal-measure strata, without any complicated downhole accidents. It has a high gas coincidence rate, wellbore stability, good inhibition performance, and uniform cuttings returned. |

**Figure 1.** Schematic diagram of the structure of the aphon.

of CGA fluids under conditions of 120~200°C and 3.5 MPa; (b) Aphrons can be used as elastic plugging materials to alleviate or avoid lost circulation. Also, aphrons have little affinity with each other or the formation rock surface, and can be easily removed by formation fluid backflow during the production stage [6,7]; (c) The construction process is simple and don't need the air compressor. Aphrons are generated by mechanical agitation of surfactants and biopolymers at a speed of higher than 5000 rpm or shearing of pipelines [8].

In theoretical research, scholars mainly focus on the aphrons stability and bubble size distribution, the rheology and plugging properties in porous media, and have obtained the following conclusive results:

- (a) In terms of the optimization of foaming agents and foam stabilizers, scholars have successively evaluated a variety of foam stabilizers (XG, starch, CMC, etc.) and multiple types of foaming agents (SDS, CTAB, X-100, CAPB [9], plant root extraction, etc.). It is proposed that the CGA system prepared by 0.3~0.8% Xanthan Gum (XG) and ~0.5% Sodium Dodecyl Sulfate (SDS) is the preferred system, with high stability and good rheology [10-15]. The polymer concentration greatly influenced the stability and bubble size of CGA fluids. The most stable CGAs were formed at higher concentrations of polymer [16];
- (b) The average size of the aphon is affected by many factors such as the type and concentration of surfactant/polymer,

temperature, pressure, agitation rate, and more. As the concentration of the foaming agent increases, the aphrons size increases; with the increase of the foam stabilizer, the size of the aphrons decreases, and the stability is significantly enhanced [17]. Alizadeh and Khamehchi established the mathematical relationship between the bubble size and temperature-pressure, and pointed out that temperature is the main factor affecting the size of aphrons [18];

- (c) In 2005, Popov and Growcock took the lead in proving that aphrons would form a plugging zone at the front of the fluid through radial flow experiments [19]; In 2012, Nareh`ei et al. pointed out that more attention should be paid to the size distribution of aphrons rather than its average size under porous media [20]; In 2019, the flow and plugging properties of CGA fluid in heterogeneous porous media were visually observed by Pasdar et al. by using the etched glass plate model and microscope [21]. By analyzing the injection pressure and backflow permeability data, it was confirmed that CGA fluid can significantly control the flow of fluid to fractures;
- (d) In terms of rheology, Arabloo and Shahri used eight kinds of rheological models to describe the rheological behavior of a typical CGA drilling fluid prepared by XG and SDS at 25~45°C, and selected the Herschel-Bulkley, Mzhari-Berk, Sisko, Power-Law and the Robertso-Stiff model [17]. Khamehchi et al. further proved that the Herschel-Bulkley model has high applicability to the CGA system, the goodness of fit is higher than 0.999 [13]. In the latest research, nanocomposite CGA fluids have attracted much attention. Herschel-Bulkley, Mzhari-Berk, Power Law, and Robertson-Stiff models' predictions have strong consistency with the experimental data of Nano-Enhanced Colloidal Gas Aphron (NCGA)-based fluids [22]. The CGA fluids have also been used as adsorbents that are easily removed from contaminated wastewater [23,24].

Table 1 lists the field application research progress of CGA drilling fluid in recent years. The CGA drilling fluid has successfully solved the problems of serious lost circulation,

reservoir damage, and difficult drilling that often occurred in drilling depleted oil/gas reservoirs and low-pressure areas. The early development of the CGA drilling fluid was mainly to optimize and compound commercial foaming agents and stabilizers to meet the needs of the site. In the past five years, the research direction has gradually changed to the independent synthesis of new treatment agents. The stability, high-temperature resistance, and anti-pollution ability of the system are improved. However, at present, the temperature resistance of CGA drilling fluid is still within 150°C, the salt resistance is $\leq 20\%$ and the calcium resistance is generally less than 1%. Further breakthroughs must be made in the aspects of high-temperature salt and calcium resistance and its environmental properties [25,26].

In this paper, a novel CGA drilling fluid system was constructed by the self-developed environment-friendly foam stabilizer EST, foaming agent AGS-8, and lubricant ChCl-PEG. A comprehensive evaluation of the stability, rheology, lubricity, filtration, anti-cuttings pollution, inhibition, environmental protection was carried out in high temperature high salt (150°C, $\leq 36\%$ NaCl) or high temperature high calcium (150°C, $\leq 7.5\%$ CaCl₂) conditions.

2. Technical requirements for CGA drilling fluids

Combined with literature research, this study puts forward the technical requirements for CGA drilling fluid.

- Stability: After high-temperature aging, the CGA drilling fluid needs to maintain good stability, which is the premise for safe drilling. In the laboratory test, the change of aphrons morphology can be observed by microscope and combined with the change of drilling fluid density, the drainage, coalescence, and defoaming of aphrons in the drilling fluid, the stability can be analyzed. Generally, one cycle of drilling fluid is usually no more than 2 h;
- Good rheology: After high-temperature aging, the drilling fluid needs to maintain good rheology to solve the problems of suspension and carrying cuttings in the drilling process, as well as keep the wellbore clean, and ensure downhole safety. Generally, it is suitable to keep the value of flow behavior index (n) at 0.4~0.7 and the value of YP/PV higher than 0.36. In addition, the LSRV is a concerned rheological parameter index in CGA drilling fluids. The LSRV value of the CGA drilling fluid system after high-temperature aging should be higher than 10000 MPas [10,27];
- Low fluid loss: Studies have shown that near/underbalanced drilling still has the possibility of filtration [28]. Therefore, the high-temperature filtration property of the CGA drilling fluid cannot be ignored, and the fluid loss volume (FL_{API}) should be controlled within 15 mL;
- The pull-up and rotation resistance of the drill string increases greatly with the increase of the well depth, and the drilling tools wear seriously during the drilling process. Drilling fluids and mud cakes need to maintain high lubricity (extreme pressure lubrication coefficient \leq

Table 2. Fundamental surfactant parameters of AGS-8.

| Sample | CMC (mmol/L) | γ_{CMC} (mN/m) | Γ_{max} (nmol/cm ²) | A_{min} (nm ²) |
|--------|-----------------|--------------------------|---|---------------------------------|
| AGS-8 | 9.69 | 38.1 | 0.15 | 1.10 |

0.20) to ensure low friction and torque, reduce sticking, and protect drilling tools [29,30];

- Inhibitory: For areas with high mudstone content, prone to collapse and clay hydration problems, the drilling fluid needs to have low fluid loss and strong inhibition to ensure wellbore stability [31];
- Cuttings resistance: Solid powder with large specific surface areas, such as cuttings, bad soil, sand, etc., will be produced during drilling. Some Solid dust will defoam or inhibit foaming. Therefore, CGA drilling fluid is also required to have a certain ability to resist cuttings pollution during on-site construction [32,33];
- Environmentally friendly: the CGA drilling fluid should not only achieve the due auxiliary drilling effect but also consider environmental protection issues, including non-toxic and easy degradation of raw material, and meeting the discharge standard and easy degradation after waste. Hence, the biodegradability and toxicity of the CGA drilling fluid system were evaluated [34].

3. Materials and method

3.1. Materials

In this paper, foam stabilizer (EST) is a graft-modified starch prepared by inverse emulsion polymerization. The synthesis method and high-temperature foam stabilization properties of EST have been reported in the previous literature [35]. EST plays the role of stabilizing foam and reducing filtration loss at a dosage of $\geq 1\%$. With the increase of EST concentration, the application effect will be enhanced. However, the dosage of EST should be controlled within 5% to avoid the adverse effect of high-concentration EST on slurry preparation.

The foaming agent is an Alkyl Glycine-type zwitterionic Surfactant (AGS-8), which is prepared with sodium chloroacetate and n-octylamine. The surface activity of AGS-8 can be referred in Table 2 and the published article for details [36]. Research has proved that AGS-8 has a good synergistic stabilization effect with EST, the high-temperature resistance is $\geq 180\text{ }^{\circ}\text{C}$, and the salt resistance reaches saturation (36% NaCl).

A Deep Eutectic Solvent (DES) ChCl-PEG synthesized by choline chloride and polyethylene glycol (PEG) was added to the system as a lubricant. DES is a new environmentally friendly, non-toxic and biodegradable solvent discovered, which usually consists of two or three kinds of Hydrogen Bond Donors (HBD) and Hydrogen Bond Acceptors (HBA) [37,38]. The HBA of ChCl-PEG is Choline Chloride (ChCl) for it contains a lot of positive charges, which is expected to form a physical adsorption film on the surface of the friction pair through electrostatic action. The

Table 3. Biodegradability of materials.

| Sample | BOD ₅ (mg/L) | COD (mg/L) | Y=BOD ₅ /COD*100 |
|----------|----------------------------|---------------|-----------------------------|
| EST | 55.8 | 168 | 33.21 |
| AGS-8 | 70.7 | 224 | 31.56 |
| ChCl-PEG | 99.2 | 285 | 34.81 |

If $Y < 5.0$, the material is difficult to degrade; If $5.0 \leq Y < 25.0$, the material is degradable; If $Y \geq 25.0$, the material is easily degradable [51].

HBD ChCl-PEG is PEG. PEG can effectively reduce the wear scar and roughness between friction pairs and is a good water-based lubricant.

As Table 3 shows, the biodegradability indexes (Y) of EST, AGS-8, and ChCl-PEG are all greater than 25, and the materials are all easily biodegradable.

3.2. Methods

3.2.1. Preparation and observation of CGA drilling fluid

CGA drilling fluid was prepared with 3% bentonite base mud, EST, AGS-8, and ChCl-PEG. First, the base mud was prepared by mixing freshwater, 0.25% Na₂CO₃, and 3% bentonite. After stirring for 1 h, the mud was stood for 16 h. Second, add EST and ChCl-PEG to the base slurry (300 mL) in turn, mix and stir at 8000 rpm for 20 min by using a high-speed mixer (Model WT-2000C, China). The polymer is fully dispersed in the base slurry. Add AGS-8 continuously and stir at 10000 rpm for 3 min to obtain the CGA drilling fluid at normal temperature. Then, CGA drilling fluid was put into a roller furnace (Model XGRL, China) and aged at 150°C for 16 h. After that, high-temperature CGA drilling fluid was obtained by stirring at 10000 rpm for 3 min again. The salt-resistance and calcium-resistance of CGA drilling fluid were evaluated by adding a certain concentration of NaCl or CaCl₂.

3.2.2. Evaluation of drilling fluid properties

Microscopic observation of aphrons: The CGA drilling fluid sample was placed on the glass slide, and the microbubbles in the system were visually observed by a polarizing microscope with CCD high-speed camera (Model Olympus BX51, Japan). The microbubbles size in the images was measured by Nano-measurer software, and then statistically analyzed in the Origin software [39].

Rheology: The rheological properties of CGA drilling fluids were studied using two viscometers. A Brookfield viscometer (Model Brookfield DV-II) was used to test the LSRV of CGA drilling fluids at 0.3 rpm. The six-speed rotational viscometer is used to test the shear stress data at different shear rates of the CGA system. Four commonly used rheological models are used to describe the rheological behavior of CGA fluid under high-temperature, high-salt, or high-calcium, and the optimal model with highest accuracy is selected [40].

$$\text{Binham model: } \tau = \tau_0 + \mu_p \gamma, \quad (1)$$

$$\text{Power-law model: } \tau = K \gamma^n, \quad (2)$$

$$\text{Casson model: } \tau^{1/2} = \tau_c^{1/2} + \eta_\infty^{1/2} \gamma^{1/2}, \quad (3)$$

$$\text{Herschel-Bulkely model: } \tau = \tau_0 + K \gamma^n, \quad (4)$$

where, τ is the shear stress; θ the reading of six-speed viscometer; γ the shear rate, τ_0 the yield point; μ_p the plastic

viscosity; K the consistency index; n the flow behavior index; τ_c the yield point of the Casson model; η_∞ the ultimate high shear viscosity; τ_0 the yield point of the H-B model.

The rheological parameters were calculated according to Eqs. (5)-(7). Stir the drilling fluid at 600 rpm for 10 s, and after standing for 10 min, multiply the maximum reading of the dial at 3 rpm by 0.511, which is the gel strength (GS₁₀ min). The ratio of YP and PV is defined as the YP/PV .

$$\text{Apparent Viscosity (AV)} = \theta_{600} \times 0.5, \quad (5)$$

$$\text{Plastic Viscosity (PV)} = \theta_{600} - \theta_{300}, \quad (6)$$

$$\text{Yield Point (YP)} = 0.511 \times (\theta_{300} - PV). \quad (7)$$

Filtration: According to the American Petroleum Institute (API) standard, the API filtration volume of CGA drilling fluid is tested in the atmosphere of 0.69 MPa N₂ by using a medium pressure fluid loss instrument (Model SD-6, China), and the filtration volume (FL_{API}) of the sample within 30 min is recorded [41].

Lubricity: The lubrication performance of drilling fluid includes the lubricity of mud cake and the lubricity of fluid. The mud cake adhesion coefficient (f) and extreme pressure lubrication coefficient (K) are the two main technical indexes to evaluate the lubricity of drilling fluid. They are evaluated by mud cake adhesion coefficient instrument (Model EP, China) and extreme pressure lubrication instrument (Model NF-2, China) respectively. The indexes are calculated according to Formulas (8)-(11) [42]:

$$\begin{aligned} \text{Adhesion coefficient (f)} &= \text{Maximum torque value (N)} \times 0.845 / 100, \quad (8) \\ &= 34 / \text{Friction coefficient with water as calibration}, \end{aligned}$$

$$\begin{aligned} \text{Correction factor (F)} &= 34 / \text{Friction coefficient with water as calibration}, \quad (9) \\ &= \text{The reading of friction coefficient} / 100, \end{aligned}$$

$$\begin{aligned} \text{Friction coefficient (M)} &= \text{The reading of friction coefficient} / 100, \quad (10) \\ &= F \times M. \end{aligned}$$

$$\text{Lubrication coefficient (K)} = F \times M. \quad (11)$$

Inhibitory: A linear dilatometer and rolling recovery experiment were used to analyze the inhibition of drilling fluid. Immerse the sample into the standard bentonite block that is pressed by the hydraulic instrument, connect the linear dilatometer and computer software, and test the expansion amount and expansion rate of the bentonite block within 16 h. Rolling recovery experiments were carried out by using a roller furnace (Model XGRL, China). Take about 20 g of sandstone rock samples (6~10 mesh) and 350 mL of drilling fluid sample into an aging jar, heat it at 150°C for 16 h. After taking out, rinse and dry, the sample was sieved with a 40-mesh sieve. Collect and weigh the cuttings that do not pass through the 40-mesh sieve, and the ratio of mass to the initial rock sample mass is the rolling recovery rate [43].

3.2.3. Environmental testing

BOD₅/COD method is an important evaluation method for the discharge and treatment of industrial wastewater containing organic matter. Dissolve the sample in deionized

Table 4. Biological toxicity classification of drilling fluid.

| Toxicity classification | Extremely high toxic | High toxic | Moderate toxic | Micro toxic | Non-toxic | Emission standard |
|-------------------------|----------------------|------------|----------------|-------------|-----------|-------------------|
| EC ₅₀ | <1 | 1~100 | 100~1000 | 1000~10000 | >10000 | >30000 |

water, and test the five-day Biochemical Oxygen Demand (BOD₅) and Chemical Oxygen Demand (COD) of the sample to evaluate the biodegradability of the material. The biodegradability evaluation index (Y) was defined as the percentage rate of BOD₅ and COD.

According to the standard “SY/T 6788-2010”, the biotoxicity test of the CGA system is carried out by the luminescent bacillus method [44]. When the luminescent ability of luminescent bacteria decreases by half, the concentration of oilfield chemicals is recorded as EC₅₀, which is used to characterize the acute toxicity level of water. The greater the EC₅₀ value, the lower the biological toxicity. The corresponding relationship between EC₅₀ and the toxicity of drilling fluid is listed in Table 4.

4. Results and discussion

4.1. Orthogonal experiment: Determining the optimal concentration of the treatment agents

A three-factor four-level orthogonal experiment was designed to determine the optimal concentration of each reagent in the formula of CGA. The high-temperature stability parameters of the system were used as the evaluation index, recording the time (T₀) when CGA begins to discharge liquid after aging at 150°C for 16 h. The results are shown in Table 5.

Based on the results of 16 sets of experiments, the average values P_1, P_2, P_3, P_4 for each factor and level were calculated, as well as the difference between the maximum average and the minimum average (range R). Results indicate that $R_A > R_B > R_C$, that is, the effects of the three reagents on the stability of the CGA system are EST, AGS-8, and ChCl-PEG in descending order. For factor A (EST dosage), $P_3 > P_4 > P_2 > P_1$, that is, when the dosage of EST is 3%, the system stability is optimal; For factor B (AGS-8 dosage), $P_1 > P_4 > P_3 > P_2$, that is, when the dosage of AGS-8 is 3%, the system stability is optimal; For factor C (ChCl PEG dosage), $P_2 > P_4 > P_3 > P_1$, that is, when the dosage of ChCl-PEG is 3%, the system stability is optimal.

Therefore, based on the high-temperature stability of the CGA drilling fluid system as the evaluation standard, the optimal formula for the CGA system was determined through orthogonal experiments as follows:

3% Bentonite mud+3% EST+3% AGS-8+3% ChCl PEG.

4.2. Bubble size distribution and stability of aphrons

The system of CGA, CGA with 36% NaCl, and CGA with 7.5% CaCl₂ are taken out after 150°C aged. After stirring at 10000 rpm for 3 min, the densities of the drilling fluid decreased from 1.03 g/cm³ to 0.78, 0.75, and 0.66 g/cm³,

respectively. Figure 2(a) and Figure 3(a) show aphrons and the bubble size distribution in the 150°C aged CGA system. Through the statistical analysis, it is found that the bubble size of aphrons in the figures is between 27.08~265.45 μm, about 87% of the aphrons have a bubble size of 10~150 μm, and the average bubble size is 99.15 μm.

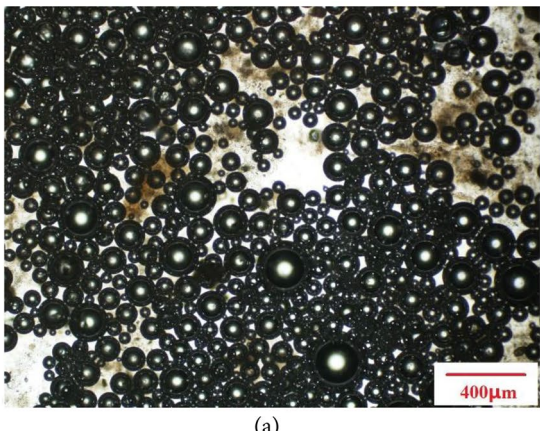
Figure 2(b) and (c) show that in the CGA system containing 36% NaCl or 7.5% CaCl₂, the aphrons always maintain a stable spherical shape with a thick liquid film, and keep independent of each other, which is highly consistent with the description of aphron structure by Sebba et al. [45]. In other words, aphrons with stable structures have been proved to be generated at high-temperature high salt, and high-temperature high calcium.

Figure 3(b) shows that the bubble size of the aphron s in the CGA system with 36% NaCl ranges from 33.86 to 266.52 μm, the proportion of aphron s in the range of 10~150 exceeds 93%, and the average diameter is 97.35 μm. Figure 3(c) shows that the bubble size of aphrons in CGA with 7.5% CaCl₂ ranges from 21.81 to 285.39 μm, the proportion in the range of 10~150 μm exceeds 96%, and the average diameter is 74.65 μm. Under the same conditions, NaCl had little effect on the density and aphron size of the CGA system. The addition of CaCl₂ increased the proportion of small-diameter microbubbles in the CGA system and decreased the average diameter.

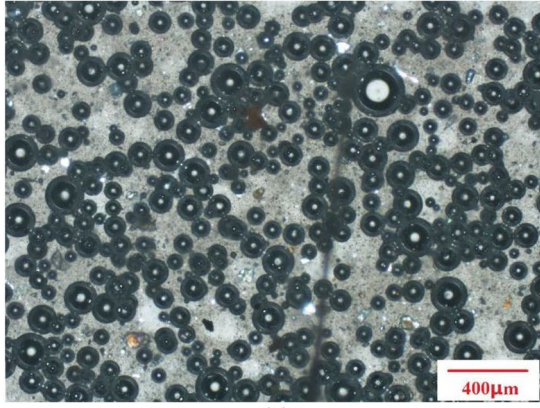
Table 5. Orthogonal experimental optimization results of CGA system.

| A: Dosage of EST | B: Dosage of AGS-8 | C: Dosage of ChCl-PEG | T ₀ (min) |
|------------------|--------------------|-----------------------|----------------------|
| 1 | 3% | 2% | 75 |
| 2 | 4% | 3% | 68 |
| 3 | 5% | 4% | 60 |
| 4 | 6% | 5% | 54 |
| 5 | 3% | 2% | 98 |
| 6 | 4% | 3% | 75 |
| 7 | 5% | 4% | 88 |
| 8 | 6% | 5% | 95 |
| 9 | 3% | 2% | 120 |
| 10 | 4% | 3% | 95 |
| 11 | 5% | 4% | 108 |
| 12 | 6% | 5% | 135 |
| 13 | 3% | 2% | 150 |
| 14 | 4% | 3% | 90 |
| 15 | 5% | 4% | 110 |
| 16 | 6% | 5% | 92 |
| P_1 | 64.25 | 110.75 | 87.5 |
| P_2 | 89 | 82 | 102.75 |
| P_3 | 114.5 | 91.5 | 91.25 |
| P_4 | 110.5 | 94 | 96.75 |
| R | 50.25 | 28.75 | 15.25 |

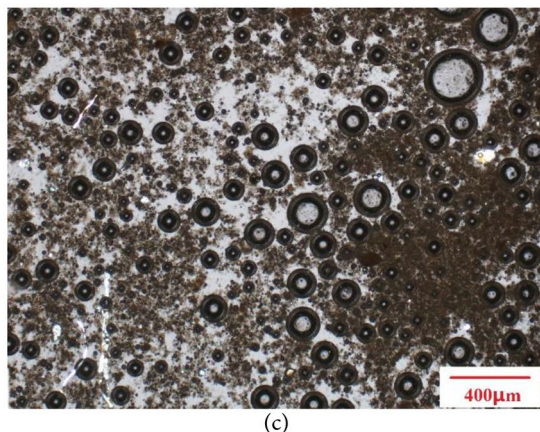
$R_A > R_B > R_C$



(a)



(b)

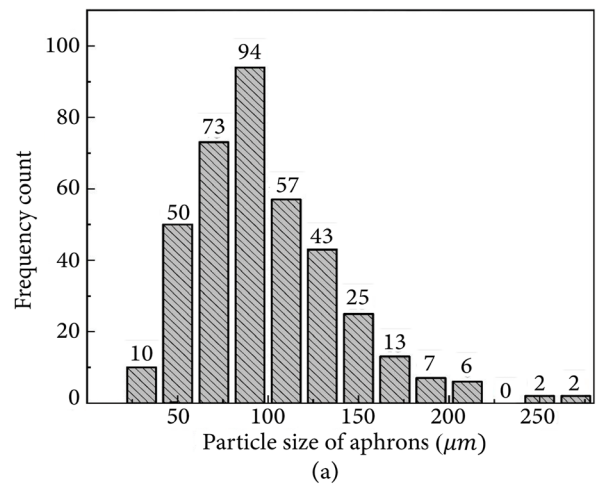


(c)

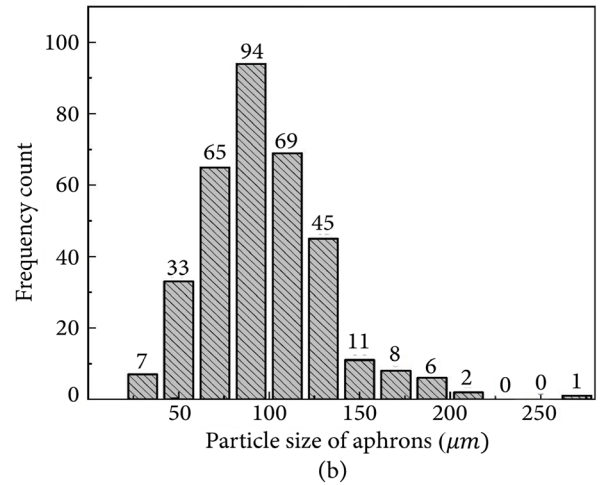
Figure 2. The figures of aaphrons in the CGA system aged at 150°C: (a) CGA; (b) CGA+36% NaCl; and (c) CGA+7.5% CaCl₂.

In general, the bubble size distribution of aaphrons in this study is highly consistent with the that of the previous reference, which intuitively proves that CGA drilling fluid is successfully generated under the conditions of high temperature, high salt, or high calcium by using EST, AGS-8, and CHCl-PEG [8].

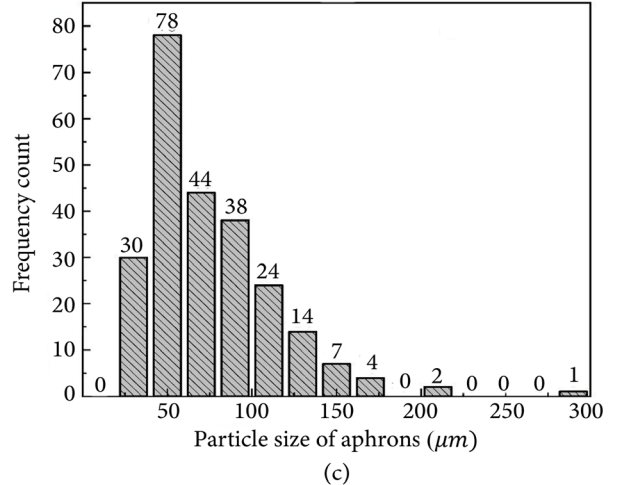
Figure 4(a), (b), and (c) show the time-dependent image of aaphrons in the CGA system, CGA containing 36% NaCl, and CGA containing 7.5% CaCl₂, respectively. The distribution of aaphrons is shown in Figure 5. There was no coalescence between foams, and no Plateau boundary in the whole observation period, which indicates that the pressure difference drainage and coalescence combination do not occur violently. As time goes by, gas diffusion takes place



(a)



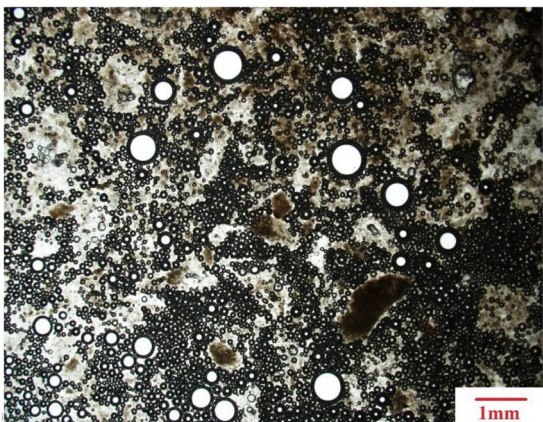
(b)



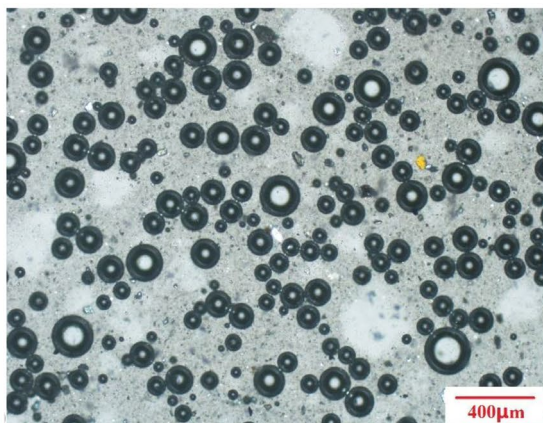
(c)

Figure 3. The bubble size distribution of aaphrons in the CGA system aged at 150°C: (a) CGA; (b) CGA+36% NaCl; and (c) CGA+7.5% CaCl₂.

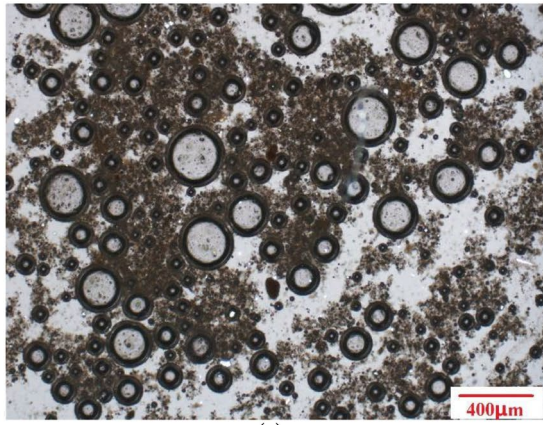
between aaphrons of different diameters. The small diameter bubble becomes smaller and smaller until it disappears, and the large diameter bubble increases. According to Table 6, the average diameters of CGA and CGA systems containing 7.5% CaCl₂ after standing for 2 h increase by 20.85 and 18.85 μm, respectively. The proportion of aaphrons with a diameter <100 μm decreased by 11.27% and 10.97%, respectively, which is within an acceptable range. The average diameter and bubble size distribution of CGA systems containing



(a)



(b)



(c)

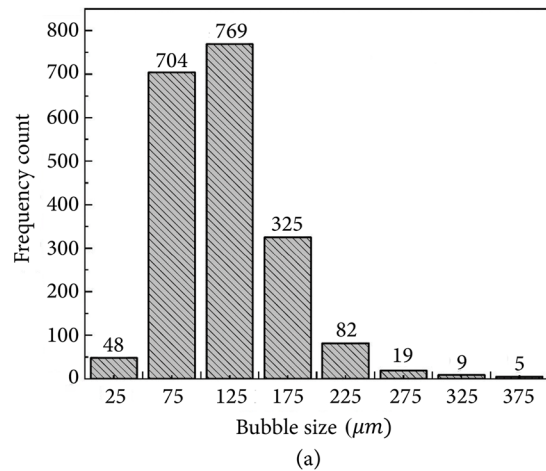
Figure 4. Observation image of Aphrons in CGA aged at 150°C after standing for 2 h (one cycle of drilling fluid): (a) CGA system; (b) CGA+36% NaCl; and (c) CGA+7.5% CaCl₂.

36% NaCl did not show significant changes. In short, the CGA system and CGA containing NaCl or CaCl₂ have high stability during an observation period of at least 2 h.

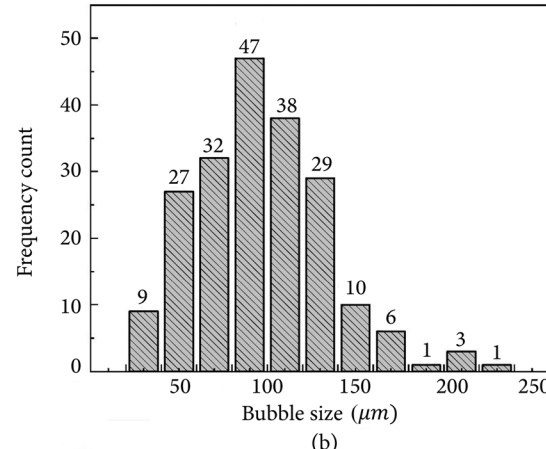
4.3. Rheology

The rheological properties of the CGA system and the CGA system containing NaCl/CaCl₂ before and after aging at 150°C were tested. The fitting results of the four rheological models were analyzed.

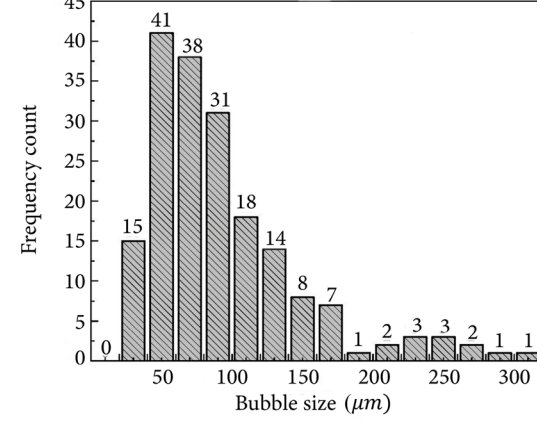
The goodness of fit value (R^2) and Root Mean Square Error (RMSE) are parameters used to evaluate fitting accuracy. The closer the R^2 value is to 1, the smaller the RMSE value, and the better the fitting of the model. As shown in



(a)



(b)



(c)

Figure 5. The bubble size distribution of aphrons in the CGA system aged at 150°C and standing for 2 h: (a) CGA; (b) CGA+36% NaCl; (c) CGA+7.5% CaCl₂.

Table 7, the Bingham model has the lowest fitting accuracy. For the CGA system under different test conditions, the value of R^2 is between 0.909 and 0.973, and the value of RMSE is high, which is between 3.07 and 7.93. The Power-law model and the Carson model have better fitting accuracy. The R^2 value of the Power-law model (0.991-1.000) is closer to 1 than that of the Carson model (0.970-0.997). But the RMSE value of the Power-law model (0.29~1.83) is higher than the Carson model.

Among the four models, the R^2 value of the Herschel-Bulkley model is greater than 0.998 and has a lower RMSE value (0.14~1.04). Therefore, the Herschel-Bulkley model is

Table 6. Data statistics of the bubble size distribution.

| Formula and conditions | Average diameter (μm) | Percentage of bubble size in the range of $<100 \mu\text{m}$ (%) | Percentage of bubble size in the range of $>100 \mu\text{m}$ (%) |
|--|------------------------------------|--|--|
| 150°C aged CGA | 99.15 | 59.16 | 40.84 |
| 150°C aged CGA—2 h | 120.00 | 47.89 | 52.11 |
| 150°C aged CGA+36% NaCl | 97.35 | 59.65 | 40.35 |
| 150°C aged CGA+36% NaCl—2 h | 96.32 | 56.16 | 43.84 |
| 150°C aged CGA+7.5% CaCl ₂ | 74.65 | 78.18 | 21.82 |
| 150°C aged CGA+7.5% CaCl ₂ —2 h | 93.50 | 67.21 | 32.79 |

Table 7. Fitting results of CGA system to four rheological models.

| Formula | Condition | Bingham model | | Power-law model | | Casson model | | Herschel-Bulkley model | |
|-------------------------|--------------|----------------------------------|----------------------|------------------------|----------------------|---------------------------------------|----------------------|--|----------------------|
| | | Fitting parameter | R ² /RMSE | Fitting parameter | R ² /RMSE | Fitting parameter | R ² /RMSE | Fitting parameter | R ² /RMSE |
| CGA | Before aging | $\tau_0=8.752$ $\mu_p=0.053$ | 0.973/3.13 | $K=1.123$ $n=0.571$ | 0.991/1.83 | $\tau_c=4.193$ $\eta_\infty=0.033$ | 0.997/0.10 | $\tau_y=4.270$ $K=0.464$ $n=0.691$ | 0.999/0.68 |
| | 150°C | $\tau_0=13.788$ $\mu_p=0.071$ | 0.941/6.29 | $K=2.448$ $n=0.503$ | 0.999/0.91 | $\tau_c=5.973$ $\eta_\infty=0.047$ | 0.984/0.29 | $\tau_y=2.809$ $K=1.723$ $n=0.550$ | 1.000/0.14 |
| +10% NaCl | Before aging | $\tau_0=8.523$ $\mu_p=0.063$ | 0.972/3.74 | $K=0.983$ $n=0.612$ | 0.996/1.39 | $\tau_c=3.441$ $\eta_\infty=0.043$ | 0.996/0.14 | $\tau_y=3.079$ $K=0.572$ $n=0.685$ | 0.999/0.58 |
| | 150°C | $\tau_0=13.193$ $\mu_p=0.074$ | 0.938/6.74 | $K=2.252$ $n=0.519$ | 1.000/0.44 | $\tau_c=5.118$ $\eta_\infty=0.052$ | 0.981/0.33 | $\tau_y=1.277$ $K=1.933$ $n=0.539$ | 1.000/0.17 |
| +20% NaCl | Before aging | $\tau_0=9.070$ $\mu_p=0.068$ | 0.966/4.50 | $K=1.122$ $n=0.604$ | 0.998/1.00 | $\tau_c=3.233$ $\eta_\infty=0.049$ | 0.991/0.23 | $\tau_y=2.163$ $K=0.799$ $n=0.649$ | 1.000/0.52 |
| | 150°C | $\tau_0=16.752$ $\mu_p=0.077$ | 0.942/6.68 | $K=3.251$ $n=0.475$ | 0.996/1.68 | $\tau_c=8.118$ $\eta_\infty=0.047$ | 0.986/0.27 | $\tau_y=5.118$ $K=1.807$ $n=0.553$ | 1.000/0.58 |
| +30% NaCl | Before aging | $\tau_0=14.021$ $\mu_p=0.060$ | 0.911/6.59 | $K=3.109$ $n=0.446$ | 0.999/0.66 | $\tau_c=6.330$ $\eta_\infty=0.038$ | 0.970/0.36 | $\tau_y=0.670$ $K=2.865$ $n=0.457$ | 0.999/0.64 |
| | 150°C | $\tau_0=13.888$ $\mu_p=0.084$ | 0.952/6.66 | $K=2.116$ $n=0.546$ | 0.998/1.30 | $\tau_c=5.497$ $\eta_\infty=0.059$ | 0.986/0.30 | $\tau_y=2.908$ $K=1.513$ $n=0.591$ | 0.999/0.80 |
| +36% NaCl | Before aging | $\tau_0=17.117$ $\mu_p=0.067$ | 0.909/7.48 | $K=4.047$ $n=0.427$ | 0.999/0.80 | $\tau_c=8.251$ $\eta_\infty=0.041$ | 0.970/0.37 | $\tau_y=1.715$ $K=3.381$ $n=0.451$ | 0.999/0.69 |
| | 150°C | $\tau_0=16.827$ $\mu_p=0.085$ | 0.934/7.93 | $K=3.112$ $n=0.494$ | 0.999/0.81 | $\tau_c=7.174$ $\eta_\infty=0.056$ | 0.981/0.35 | $\tau_y=2.538$ $K=2.409$ $n=0.528$ | 1.000/0.22 |
| +5% CaCl ₂ | Before aging | $\tau_0=13.100$ $\mu_p=0.055$ | 0.927/5.41 | $K=2.871$ $n=0.445$ | 0.997/1.00 | $\tau_c=6.381$ $\eta_\infty=0.033$ | 0.977/0.30 | $\tau_y=2.882$ $K=1.892$ $n=0.500$ | 0.999/0.64 |
| | 150°C | $\tau_0=7.258$ $\mu_p=0.062$ | 0.963/4.26 | $K=0.885$ $n=0.622$ | 1.000/0.29 | $\tau_c=2.102$ $\eta_\infty=0.048$ | 0.989/0.25 | $\tau_y=0.620$ $K=0.796$ $n=0.636$ | 1.000/0.15 |
| +7.5% CaCl ₂ | Before aging | $\tau_0=7.464$ $\mu_p=0.042$ | 0.959/3.07 | $K=1.097$ $n=0.543$ | 0.993/1.26 | $\tau_c=3.448$ $\eta_\infty=0.027$ | 0.993/0.14 | $\tau_y=2.844$ $K=0.557$ $n=0.634$ | 0.998/0.69 |
| | 150°C | $\tau_0=5.281$ $\mu_p=0.059$ | 0.971/3.63 | $K=0.549$ $n=0.684$ | 0.998/1.04 | $\tau_c=1.213$ $\eta_\infty=0.049$ | 0.991/0.22 | $\tau_y=0.203$ $K=0.528$ $n=0.689$ | 0.998/1.04 |

the optimal model to describe the rheological behavior of the CGA system.

Table 8 lists the rheological parameters of the CGA system. The results show that the Apparent Viscosity (AV) and Plastic Viscosity (PV) of the CGA system increase with the increase of NaCl before and after aging at 150°C. The YP/PV of the CGA system with different concentrations of NaCl fluctuated

between 0.456 and 0.772, and was always higher than 0.36. The flow behavior index (n) was between 0.451 and 0.691. At this time, the drilling fluid has a high cuttings-carrying capacity and strong shear-thinning properties.

The addition of CaCl₂ reduced the viscosity of the system to a certain extent after high-temperature aging. The values of AV and PV of the CGA system containing CaCl₂ before and after

Table 8. Rheological parameters of CGA system with different concentrations of NaCl/CaCl₂ before and after aging at 150°C.

| Formula | Condition | LSRV (mPa·s) | GS _{10min} (Pa) | n | AV (mPa·s) | PV (mPa·s) | YP (Pa) | YP/PV |
|------------------------------|--------------|-----------------|-----------------------------|-------|---------------|---------------|------------|-------|
| CGA-2 | Before aging | 84583 | 7.154 | 0.691 | 59.5 | 39 | 20.951 | 0.537 |
| | 150°C/16h | 51189 | 7.665 | 0.550 | 80.5 | 49 | 32.193 | 0.657 |
| CGA-2+10% NaCl | Before aging | 63394 | 6.132 | 0.685 | 68.5 | 47 | 21.973 | 0.468 |
| | 150°C/16h | 38995 | 5.621 | 0.539 | 82.5 | 51 | 32.193 | 0.631 |
| CGA-2+20% NaCl | Before aging | 63995 | 5.621 | 0.649 | 74 | 51 | 23.506 | 0.461 |
| | 150°C/16h | 39995 | 8.176 | 0.553 | 89 | 56 | 33.726 | 0.602 |
| CGA-2+30% NaCl | Before aging | 71790 | 7.665 | 0.457 | 69 | 40 | 29.638 | 0.741 |
| | 150°C/16h | 42796 | 6.132 | 0.591 | 94 | 65 | 29.638 | 0.456 |
| CGA-2+36% NaCl | Before aging | 75392 | 9.198 | 0.451 | 79 | 45 | 34.748 | 0.772 |
| | 150°C/16h | 46595 | 6.132 | 0.528 | 96 | 57 | 39.858 | 0.699 |
| CGA-2+5% CaCl ₂ | Before aging | 47991 | 7.665 | 0.500 | 64 | 38 | 26.572 | 0.699 |
| | 150°C/16h | 36195 | 5.11 | 0.636 | 66 | 46 | 20.440 | 0.444 |
| CGA-2+7.5% CaCl ₂ | Before aging | 38500 | 6.132 | 0.634 | 47.5 | 30 | 17.885 | 0.596 |
| | 150°C/16h | 29393 | 5.11 | 0.689 | 62 | 42 | 20.440 | 0.487 |

Table 9. Filtration and lubricity of CGA system with different concentrations of NaCl/CaCl₂ before and after aging at 150°C.

| Formula | Condition | FL _{API} (mL) | Adhesion coefficient | Lubrication coefficient |
|----------------------------|--------------|------------------------|----------------------|-------------------------|
| CGA | Before aging | 6.2 | 0.057 | 0.116 |
| | 150°C/16 h | 4.2 | 0.063 | 0.122 |
| CGA+10% NaCl | Before aging | 6 | 0.059 | 0.120 |
| | 150°C/16 h | 4.5 | 0.078 | 0.132 |
| CGA+20% NaCl | Before aging | 6 | 0.068 | 0.117 |
| | 150°C/16 h | 3.5 | 0.073 | 0.122 |
| CGA+30% NaCl | Before aging | 5.5 | 0.072 | 0.108 |
| | 150°C/16 h | 3 | 0.076 | 0.114 |
| CGA+36% NaCl | Before aging | 4.8 | 0.073 | 0.104 |
| | 150°C/16 h | 2.5 | 0.086 | 0.107 |
| CGA+5% CaCl ₂ | Before aging | 6.5 | 0.097 | 0.098 |
| | 150°C/16 h | 4 | 0.097 | 0.113 |
| CGA+7.5% CaCl ₂ | Before aging | 5.4 | 0.100 | 0.102 |
| | 150°C/16 h | 3.5 | 0.123 | 0.116 |

aging at 150°C remained above 47.5 MPa·s and 30 MPa·s, respectively. The value of YP/PV (0.444~0.699) and n (0.500~0.689) both fluctuated within appropriate ranges.

In addition, the CGA system always has higher gel strength ($GS_{10min}>5.11$ Pa) and low shear viscosity ($LSRV>29393$ MPa·s) under different conditions. To sum up, the CGA system has appropriate rheological parameters and high LSRV values under high temperature, high salt and high calcium environment, which shows high cuttings-carrying ability and strong shear-thinning behavior.

4.4. Filtration and lubricity

Table 9 lists the filtration and lubricity parameters of CGA and CGA systems containing different concentrations of

NaCl and CaCl₂ before and after aging at 150°C. The CGA system maintains a stable low filtration volume under the condition of a high concentration of NaCl/CaCl₂. With the increase of NaCl/CaCl₂, the FL_{API} of CGA at room temperature fluctuates in the range of 4.8~6.5 mL. After 150°C aging, the filtration property of the CGA system is slightly improved, and the FL_{API} fluctuates within 2.5~4.5 mL, which always meets the API requirements [46]. In addition, a low value of fluid loss minimizes hydration expansion and maintains formation stability when drilling into mudstone formations.

With the increase of NaCl/CaCl₂, the lubrication coefficient of the CGA system decreased, and the adhesion coefficient of the mud cake increased slightly. In general,

Table 10. Cuttings resistance of CGA.

| Formula | LSRV (mPa·s) | GS _{10min} (Pa) | AV (mPa·s) | PV (mPa·s) | YP (Pa) | YP/PV | FLAPI (mL) | f | K |
|------------------|-----------------|-----------------------------|---------------|---------------|------------|-------|------------|-------|-------|
| CGA | 51189 | 7.665 | 80.5 | 49 | 32.19 | 0.657 | 4.2 | 0.063 | 0.122 |
| CGA+5%Cuttings | 56796 | 6.132 | 71 | 42 | 29.64 | 0.706 | 5.2 | 0.106 | 0.155 |
| CGA+10% Cuttings | 61394 | 7.154 | 89 | 49 | 40.88 | 0.834 | 6.2 | 0.112 | 0.191 |
| CGA+15% Cuttings | 61993 | 12.264 | 112.5 | 75 | 38.33 | 0.511 | 4.6 | 0.152 | 0.246 |

Table 11. Inhibition performance of various drilling fluid systems.

| Formula | Linear expansion rate (%) | Rolling recovery rate (%) |
|--|------------------------------|------------------------------|
| CGA | 5.63 | 87.98% |
| CGA+36% NaCl | 6.24 | 84.94% |
| CGA+7.5% CaCl ₂ | 4.29 | 84.26% |
| Water-based drilling fluids based on KCl, polymers, amine-based polyalcohols and nano-wetting modifiers [52] | 6.6~7.2 | 80.8~85.5 |
| Solid-free low damage and strong inhibition water-based drilling fluid system [53] | ~5 | 85.33 |

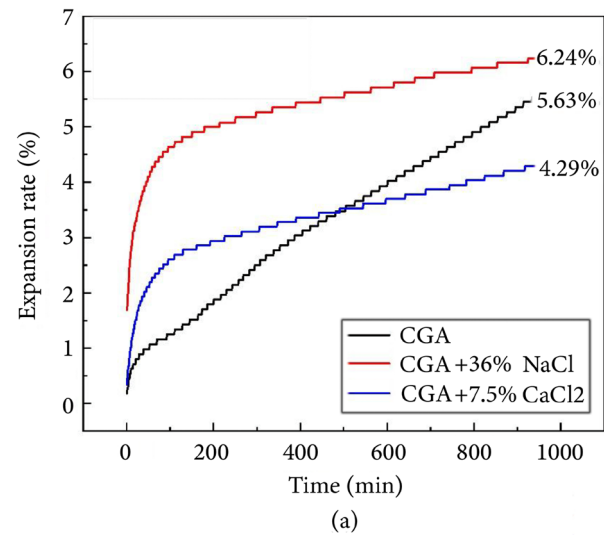
with different concentrations of ion contamination, the CGA system maintained a low adhesion coefficient (0.057~0.123) and lubrication coefficient (0.098~0.132) before and after high-temperature aging. In summary, CGA has good filtration properties and lubricity under conditions of high temperature, high salt, and high calcium.

4.5. Cuttings resistance

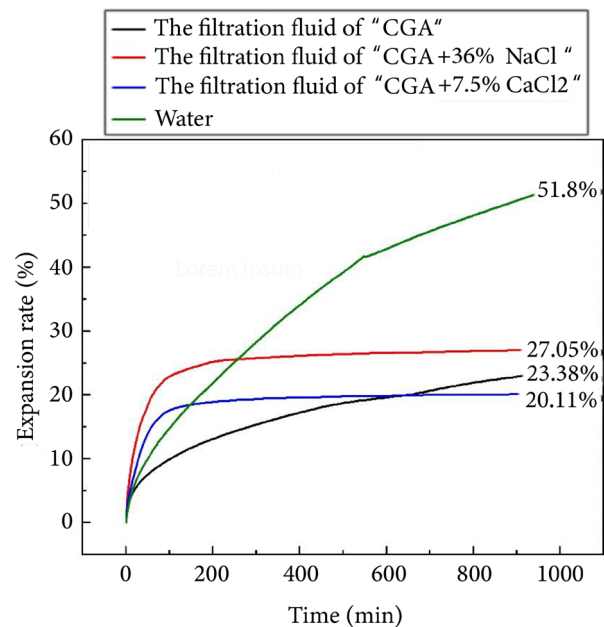
Add 5%, 10%, and 15% cuttings to the CGA system in turn, and the property changes after aging at 150°C for 16 h are shown in Table 10. After adding 5% or 10% cuttings, the viscosity and GS_{10 min} changed within an acceptable range, the fluid loss increased slightly, and the lubricity decreased. In general, all parameters met the design requirements. The 15% cuttings significantly reduced the performance of the drilling fluid. The dispersion of rock powder led to a significant increase in the AV and PV. The AV and PV values of the CGA system reached 112.5 and 75 MPas, respectively, which may lead to difficulty in pump starting and solid-phase removing. In addition, the lubrication coefficient of the CGA system is also far beyond the design requirements. In conclusion, the anti-cuttings pollution ability of CGA after aging at 150°C is not less than 10%.

4.6. Inhibitory

As shown in Figure 6(a), CGA drilling fluid always maintains a low linear expansion rate (4.29~6.24%) at high-temperature or high-concentration ion pollution, which is equivalent to a variety of strongly inhibitory water-based drilling fluid systems (Table 11). The filtration fluid of the CGA system is also obtained with the medium-pressure filtration instrument. The linear expansion rates of freshwater and filtration fluid are tested and compared, which is more in line with the actual drilling conditions. As shown in Figure 6(b), the bentonite block has a significant hydration expansion in the freshwater, with an expansion rate of 51.8%. While the expansion rate of the filtration fluid of



(a)



(b)

Figure 6. Curves of “expansion rate-time” of CGA system aged at 150°C: (a) CGA drilling fluid and (b) the filtration fluid of CGA drilling fluid.

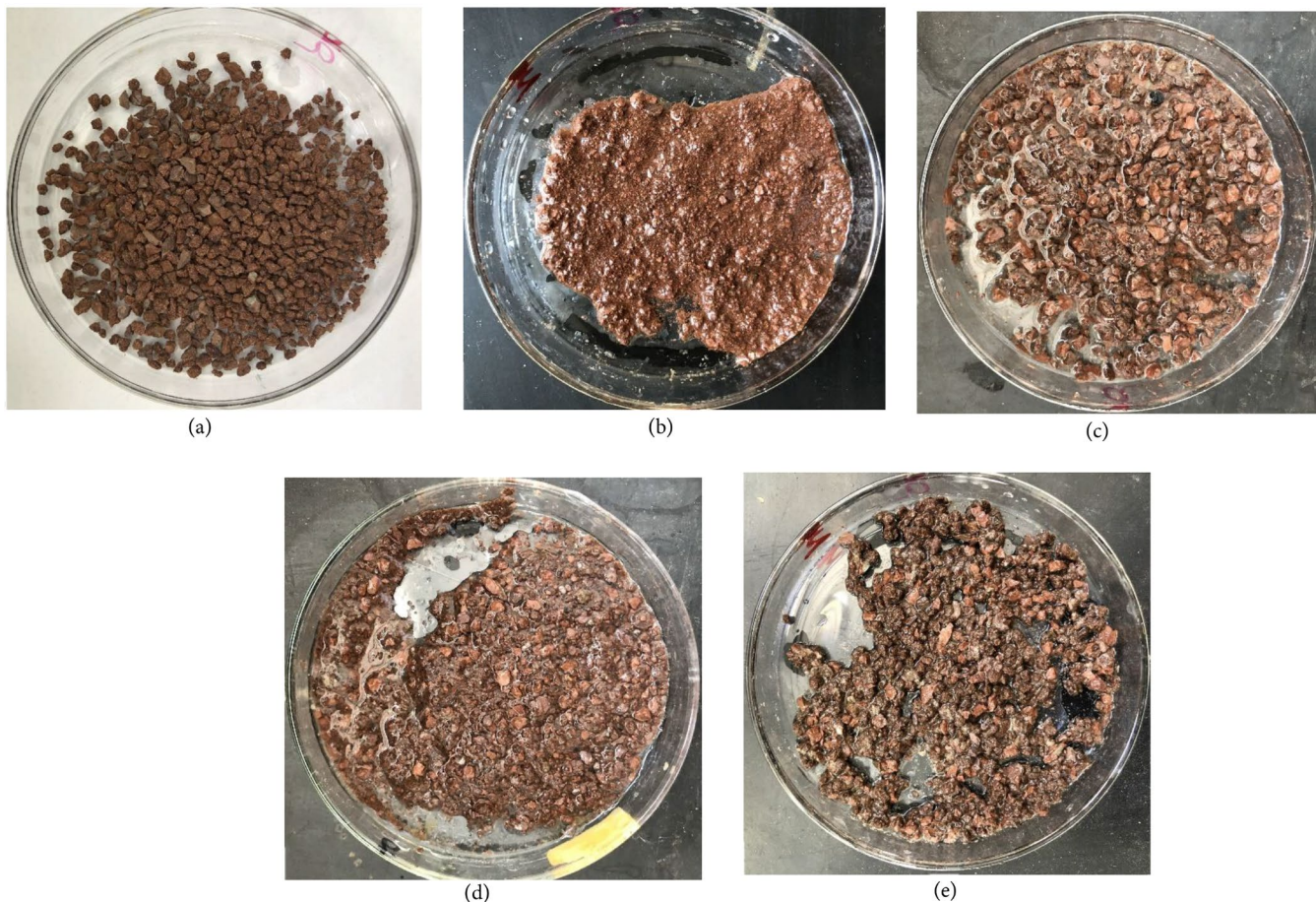


Figure 7. Sandstone samples from rolling recovery experiments: (a) Initial samples; (b) After boiling in water; (c) After hot rolling in the CGA system; (d) After hot rolling in CGA+36% NaCl; (e) After hot rolling in CGA+7.5% CaCl₂.

CGA, CGA+36% NaCl, and CGA+7.5% CaCl₂ system, which is between 20.11~27.05%. Therefore, the CGA system has good inhibition properties and compatibility with easily hydrated formation.

According to the rolling recovery experiment (Figure 7), the sandstone particles in freshwater are broken and become fine after hot rolling at 150°C for 16 h. Most of the particles with a particle size of more than 40 mesh are screened out, and the rolling recovery rate is only 43.41%. In the CGA system, the cuttings recovered after aging still maintain a good coarse particle shape and have a high recovery rate (87.98%). The rolling recovery rate of the CGA system with 36% NaCl or 7.5% CaCl₂ decreases slightly but remains at a high value (84.94% and 84.26%).

Combined with Table 11 and the test results, it can be found that the inhibition of the CGA system is equivalent to a variety of strongly inhibitory water-based drilling fluids. The CGA system has excellent inhibition at high temperature, high salt, and high calcium conditions, and is suitable for collapse-prone formations like shale or loose sandstone.

4.7. Environmental testing

The biodegradability of the CGA system was tested by the BOD₅/COD method. Results show that the BOD₅ and COD

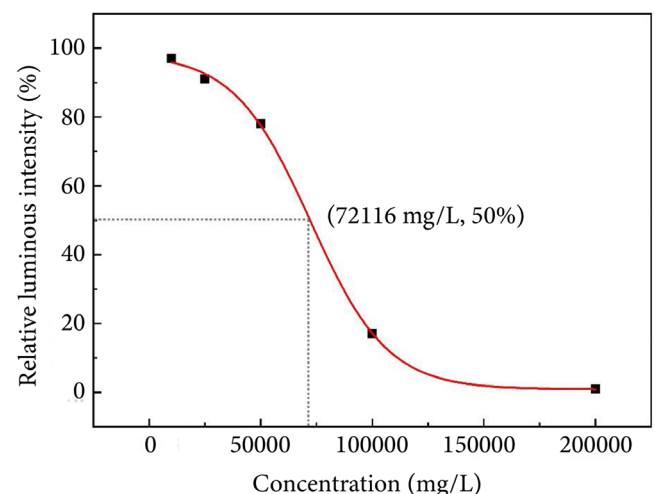


Figure 8. The biological toxicity test of CGA system.

value of CGA drilling fluid is 66.3 mg/L and 209 mg/L, respectively. The biodegradability evaluation index (Y) was 31.72. Therefore, the CGA system is biodegradable.

Figure 8 shows the “Concentration-Relative luminous intensity” curve of the filtration fluid of the CGA system. The EC₅₀ value is 72116 mg/L. Based on Table 3, it can be determined that the CGA system is an environmental-friendly and non-toxic drilling fluid system.

5. Conclusion

This study constructs a Colloidal Gas Aphron (CGA) drilling fluid system with high-temperature resistance (150°C), salt-resistance, and calcium-resistance (36% NaCl or 7.5% CaCl₂). The stability, rheology, filtration, lubricity, anti-cuttings pollution ability, inhibition, and biological toxicity of the CGA system were evaluated. The following conclusions can be drawn:

- Using the high-temperature stability of the CGA system as an indicator, the formula of the CGA system was optimized through three-factors four-levels orthogonal experiments, which is: 3% Bentonite mud+3% EST+3% AGS-8+3% ChCl PEG;
- Microscopic tests showed that stable aphrons were successfully generated in 36% NaCl-CGA or 7.5% CaCl₂-CGA system aged at 150°C. Aphrons maintain a stable morphology throughout a 2 h observation period without significant coalescence;
- The Herschel-Bulkley model accurately describes the rheological behavior of CGA fluids containing NaCl/CaCl₂. The addition of NaCl increases the viscosity of the CGA fluid, while CaCl₂ is the opposite. The CGA fluid maintains appropriate rheological parameters (fluidity index, gel strength, and yield point) and shear thinning behavior, which means good cuttings carrying capacity;
- With the addition of NaCl/CaCl₂, the CGA has a low filtration volume (<7 mL) and low value of lubrication coefficient (0.107~0.132), which meets API requirements of filtration and lubricity properties;
- The anti-cuttings pollution ability of 150°C aged CGA can reach 10%. CGA, 36% NaCl-CGA, and 7.5% CaCl₂-CGA all have low linear expansion rates (<28%) and high rolling recovery rates (>84%). The CGA system has good inhibitory performance and is compatible with sandstone, shale and other easily collapsed formations;
- The CGA system has been proven to be a biodegradable and non-toxic drilling fluid system.

In summary, this study breaks through the limitations of high temperature, high salinity, and high calcium conditions on the CGA properties, providing possibilities for the application of CGA drilling fluids in complex formations.

Nomenclature

| | |
|-------------------|--|
| AGS-8 | An amino acid foaming agent |
| API | American Petroleum Institute |
| AV | Apparent Viscosity |
| BOD ₅ | The five-day Biochemical Oxygen Demand |
| CaCl ₂ | Calcium Chloride |
| CGA | Colloidal Gas Aphron |
| ChCl-PEG | Lubricant |
| CAPB | Coconut oil Amide Propyl Betaine |
| CMC | Carboxymethyl Cellulose |
| COD | Chemical Oxygen Demand |
| CTAB | Cetyltrimethylammonium bromide |

| | |
|-----------------------|---|
| EC ₅₀ | The concentration of oilfield chemicals in the biological toxicity test |
| EST | A modified starch foam stabilizer |
| <i>f</i> | The mud cake adhesion coefficient |
| FL _{API} | Filtration volume |
| GS _{10min} | 10 minutes gel strength |
| HTHP | High Temperature High Pressure |
| <i>k</i> | The extreme Pressure lubrication coefficient |
| LSRV | Low Shear Rate Viscosity |
| <i>n</i> | The flow behavior index |
| <i>R</i> ² | The goodness of fit value |
| ROP | The borehole footage per unit time |
| RMSE | Root Mean Square Error |
| SDS | Sodium Dodecyl Sulfate |
| XG | Xanthan Gum |
| X-100 | Triton X-100 |
| YP | Yield Point |
| τ | The shear stress |
| θ | The reading of six-speed viscometer |
| γ | The shear rate |
| τ_0 | The yield point of Bingham model |
| μ_p | The plastic viscosity |
| τ_c | The yield point of the Casson model |
| η_∞ | The ultimate high shear viscosity |
| τ_y | The yield point of the H-B model |
| γ_{CMC} | Surface tension corresponding to the critical micelle concentration |
| Γ_{max} | The saturated adsorption capacity |
| A_{min} | The minimum surface area |

Acknowledgments

This research has been funded by the Natural Science Foundation of Henan Province-Youth Science Foundation Project (252300420834) and Key Scientific Research Project of Higher Education Institutions in Henan Province (25B440001).

Conflicts of interest

The authors declare that they have no known competing financial interests or personal relationships that could have appeared to influence the work reported in this paper.

Authors contribution statement

First author: Data curation; Formal analysis; Writing – original draft

Second author: Investigation; Software

Third author: Writing – review and editing

References

1. Hosseini-Kaldozakh, S.A., Khamehchi, E., Dabir, B., et al. “Rock wettability effect on colloidal gas aphron invasion near wellbore region”, *J. Petrol. Sci. Eng.*, **189**, 106766 (2020).
<https://doi.org/10.1016/j.petrol.2019.106766>

2. Growcock, F.B., Belkin, A., Fosdick, M., et al. "Recent advances in aphron drilling-fluid technology", *SPE Drilling & Completion*, **22**(2), pp. 74-80 (2007).
<https://doi.org/10.2118/97982-PA>
3. Jianyu, X., Yaxian, Z., Xiaohui, G., et al. "Laboratory study and performance evaluation on micro-foam drilling fluid", *Advances in Fine Petrochemicals*, **15**(4), pp. 30-34 (2014).
<https://doi.org/10.4028/www.scientific.net/AMR.868.601>
4. Pasdar, M., Kazemzadeh, E., Kamari, E., et al. "Insight into the behavior of colloidal gas aphron (CGA) fluids at elevated pressures: an experimental study", *Colloids and Surfaces a-Physicochemical and Engineering Aspects*, **537**, pp. 250-258 (2018).
<https://doi.org/10.1016/j.colsurfa.2017.10.001>
5. Zhu, W. and Zheng, X. "High temperature sealing performance of novel biodegradable colloidal gas aphron (CGA) drilling fluid system", *J. Japan Petrol. Inst.*, **64**(6), pp. 1-9 (2021).
<https://doi.org/10.1627/jpi.64.331>
6. Molaei, A. and Waters, K.E. "Aphron applications-a review of recent and current research", *Adv. Colloid Interface Sci.*, **216**, pp. 36-54 (2015).
<https://doi.org/10.1016/j.cis.2014.12.001>
7. Belkin, A., Irving, M., Connor, B., et al. "How aphron drilling fluids work", *SPE Annual Technical Conference and Exhibition* (2005).
<https://doi.org/10.2523/96145-MS>
8. Huaidong, L., Libao, S., Jingjie, Z., et al. "Recyclable micro foam drilling fluid: its study and application in burial hill structure in Chad", *Drilling Fluid & Completion Fluid*, **34**(5), pp. 8-13 (2017).
<https://doi.org/10.3969/j.issn.1001-5620.2017.05.002>
9. Keshavarzi, B., Javadi, A., Bahramian, A., et al. "Formation and stability of colloidal gas aphron based drilling fluid considering dynamic surface properties", *J. Japan Petrol. Inst.*, **174**, pp. 468-475 (2019).
<https://doi.org/10.1016/j.petrol.2018.11.057>
10. Tabzar, A., Arabloo, M., and Ghazanfari, M.H. "Rheology, stability and filtration characteristics of colloidal gas aphron fluids: role of surfactant and polymer type", *J. Nat. Gas. Sci. Eng.*, **26**, pp. 895-906 (2015).
<https://doi.org/10.1016/j.jngse.2015.07.014>
11. Bjordalen, N. and Kuru, E. "Physico-chemical characterization of aphron-based drilling fluids", *J. Can. Pet. Technol.*, **47**(11), pp. 15-21 (2008).
<https://doi.org/10.2118/08-11-15-CS>
12. Ahmadi, M.A., Galedarzadeh, M., and Shadizadeh, S.R. "Colloidal gas aphron drilling fluid properties generated by natural surfactants: experimental investigation", *J. Nat. Gas. Sci. Eng.*, **27**, pp. 1109-1117 (2015).
<https://doi.org/10.1016/j.jngse.2015.09.056>
13. Khamehchi, E., Tabibzadeh, S., and Alizadeh, A. "Rheological properties of aphron based drilling fluids", *Petroleum Exploration and Development*, **43**(6), pp. 1076-1081 (2016).
[https://doi.org/10.1016/S1876-3804\(16\)30125-2](https://doi.org/10.1016/S1876-3804(16)30125-2)
14. Zhu, W., Zheng, X., Li, G., et al. "Impact of foaming agent on the performance of colloidal gas aphron drilling fluid for geothermal drilling", *Geothermal Resources Council 2019 Annual Meeting - Geothermal: Green Energy for the Long Run, GRC 2019*, **8**(48), pp. 349-358 (2019).
<https://doi.org/10.1021/acsomega.3c07131>
15. Heidari, M., Shahbazi, K., and Fattahi, M. "Experimental study of rheological properties of aphron based drilling fluids and their effects on formation damage", *Sci. Iranica*, **24**(3), pp. 1241-1252 (2017).
<https://doi.org/10.24200/sci.2017.4108>
16. Pasdar, M., Kazemzadeh, E., Kamari, E., et al. "Insight into selection of appropriate formulation for colloidal gas aphron (CGA)-based drilling fluids", *Petroleum Science*, **17**(3), pp. 759-767 (2020).
<https://doi.org/10.1007/s12182-020-00435-z>
17. Arabloo, M. and Shahri, M.P. "Experimental studies on stability and viscoplastic modeling of colloidal gas aphron (CGA) based drilling fluids", *J. Japan Petrol. Inst.*, **113**, pp. 8-22 (2014).
<https://doi.org/10.1016/j.petrol.2013.12.002>
18. Alizadeh, A. and Khamehchi, E. "Mathematical modeling of the colloidal gas aphron motion through porous medium, including colloidal bubble generation and destruction", *Colloid. Polym. Sci.*, **294**(6), pp. 1075-1085 (2016).
<https://doi.org/10.1007/s00396-016-3866-y>
19. Popov, P. and Growcock, F.B. "Effectiveness of aphron drilling fluids in depleted zones", *Drilling Contractor*, **61**(3), pp. 55-58 (2005).
<https://doi.org/10.4043/14278-MS>
20. Nareh`ei, M.A., Shahri, M.P., and Zamani, M. "Preparation and characterization of colloidal gas aphron based drilling fluids using a plant-based surfactant", *SPE Saudi Arabia Section Technical Symposium and Exhibition* (2012).
<https://doi.org/10.2118/160888-MS>
21. Pasdar, M., Kamari, E., Kazemzadeh, E., et al. "Investigating fluid invasion control by colloidal gas aphron (CGA) based fluids in micromodel systems", *J. Nat. Gas. Sci. Eng.*, **66**, pp. 1-10 (2019).
<https://doi.org/10.1016/j.jngse.2019.03.020>
22. Tabzar, A., Ziae, H., Arabloo, M., et al. "Physicochemical properties of nano-enhanced colloidal gas aphron (NCGA)-based fluids", *European Physical Journal Plus*, **135**(3), 312 (2020).
<https://doi.org/10.1140/epjp/s13360-020-00174-5>

23. Ghafelebashi, A., Khosravani, S., Kazemi, M.H., et al. “A novel fabricated polyvinyl alcohol/ bentonite nanocomposite hydrogel generated into colloidal gas aphon”, *Colloids and Surfaces a-Physicochemical and Engineering Aspects*, **650**, 129580 (2022).
<https://doi.org/10.1016/j.colsurfa.2022.129580>

24. Mo, Y., Dong, J., Fan, Y., et al. “Stability and migration characteristics of SDS and SiO₂ colloidal gas aphon and its removal efficiency for nitrobenzene-contaminated aquifers”, *J. Environ. Eng.*, **149**(4), pp. 1-11 (2023).
<https://doi.org/10.1061/JOEEDU.EEENG-7124>

25. Liu, J., Dai, Z., Xu, K., et al. “Water-based drilling fluid containing bentonite/poly(sodium 4-styrenesulfonate) composite for ultrahigh-temperature ultradeep drilling and its field performance”, *Spe Journal*, **25**(3), pp. 1193-1203 (2020).
<https://doi.org/10.2118/199362-PA>

26. Gautam, S. and Guria, C. “Optimal synthesis, characterization, and performance evaluation of high-pressure high-temperature polymer-based drilling fluid: the effect of viscoelasticity on cutting transport, filtration loss, and lubricity”, *Spe Journal*, **25**(3), pp. 1333-1350 (2020).

27. Li, W., Zhao, X., Ji, Y., et al. “Investigation of biodiesel-based drilling fluid, Part 2: formulation design, rheological study, and laboratory evaluation”, *Spe Journal*, **21**(5), pp. 1767-1781 (2016).
<https://doi.org/10.2118/180926-PA>

28. Ding, Y., Herzhaft, B., and Renard, G. “Near-wellbore formation damage effects on well performance-a comparison between underbalanced and overbalanced drilling”, *SPE International Symposium and Exhibition on Formation Damage Control* (2004).
<https://doi.org/10.2118/86558-PA>

29. Livescu, S. and Craig, S. “Increasing lubricity of downhole fluids for coiled-tubing operations”, *Spe Journal*, **20**(2), pp. 396-404 (2015).
<https://doi.org/10.2118/168298-PA>

30. Livescu, S., Craig, S., and Aitken, B. “Fluid-hammer effects on coiled-tubing friction in extended-reach wells”, *Spe Journal*, **22**(1), pp. 365-373 (2017).
<https://doi.org/10.2118/179100-PA>

31. Ma, J., Yu, P., Xia, B., et al. “Synthesis of a biodegradable and environmentally friendly shale inhibitor based on chitosan-grafted l-arginine for wellbore stability and the mechanism study”, *ACS Applied Bio Materials*, **2**(10), pp. 4303-4315 (2019).
<https://doi.org/10.1021/acsabm.9b00566>

32. Rehman, S.R.U., Zahid, A.A., Hasan, A., et al. “Experimental investigation of volume fraction in an annulus using electrical resistance tomography”, *Spe Journal*, **24**(5), pp. 1947-1956 (2019).

33. Song, X., Pang, Z., Xu, Z., et al. “Experimental study on the sliding friction for coiled tubing and high-pressure hose in a cuttings bed during microhole-horizontal-well drilling”, *Spe Journal*, **24**(5), pp. 2010-2019 (2019).

34. Quintero, L., Limia, J.M., and Stocks-Fischer, S. “Silica micro-encapsulation technology for treatment of oil and/or hydrocarbon-contaminated drill cuttings”, *Spe Journal*, **6**(1), pp. 57-60 (2001).
<https://doi.org/10.2118/69675-PA>

35. Zhu, W., Zheng, X., Shi, J., et al. “Grafted starch foam stabilizer ESt-g-NAA for high-temperature resistant CGA drilling fluid via inverse emulsion polymerization”, *Starch-Starke*, **73**(9-10), pp. 1-15 (2021).
<https://doi.org/10.1002/star.202000240>

36. Zhu, W. and Zheng, X. “Study of an anti-high-temperature and salt-resistance alkyl glycine foaming agent and its foam stabilizing mechanism”, *J. Disper. Sci. Technol.*, **44**(4), pp. 86-97 (2021).
<https://doi.org/10.1080/01932691.2021.1931282>

37. Wu, K., Su, T., Hao, D., et al. “Choline chloride-based deep eutectic solvents for efficient cycloaddition of CO₂ with propylene oxide”, *ChCom*, **54**(69), pp. 9579-9582 (2018).
<https://doi.org/10.1039/C8CC04412>

38. Chao, Y., Ding, H., Pang, J., et al. “High efficient extraction of tryptophan using deep eutectic solvent-based aqueous biphasic systems”, *Indian J. Pharm. Sci.*, **81**(3), pp. 448-455 (2019).
<https://doi.org/10.36468/pharmaceutical-sciences.529>

39. Zhu, W., Zheng, X., and Li, G. “Micro-bubbles size, rheological and filtration characteristics of Colloidal Gas Aphron (CGA) drilling fluids for high temperature well: role of attapulgite”, *J. PETROL. SCI. ENG*, **186**, pp. 1-11 (2020).
<https://doi.org/10.1016/j.petrol.2019.106683>

40. Nareh'e, M.A., Shahri, M.P., Zamani, M. “Rheological and filtration loss characteristics of colloidal gas aphon based drilling fluids”, *J. Japan Petrol. Inst.*, **55**(3), pp. 182-190 (2012).
<https://doi.org/10.1627/jpi.55.182>

41. Zhu, W. and Zheng, X. “Effective modified Xanthan gum fluid loss agent for high temperature water-based drilling fluid and the filtration control mechanism”, *ACS Omega*, **6**(37), pp. 23788-23801 (2021).
<https://doi.org/10.1021/acsomega.1c02617>

42. Zhang, T., Cui, B., Xue, W., et al. “Preparation and applications of an advanced lubricant for brine water-based drilling fluids”, *7th International Conference on Education, Management, Computer and Society (EMCS)*, pp. 1898-1908 (2017).
<https://doi.org/10.2991/emcs-17.2017.360>

43. Su, J., Liu, M., Lin, L., et al. “Sulfonated lignin modified with silane coupling agent as biodegradable shale

inhibitor in water-based drilling fluid”, *J. Petrol. Sci. Eng.*, **208**, 109618 (2022).
<https://doi.org/10.1016/j.petrol.2021.109618>

44. Evaluation method for environmental protection technology of water-soluble oilfield chemicals. Petroleum Standards, (2010).

45. Sebba, F., *Foams and Biliqid Foams-Aphrons*, New York: Wiley (1987).
<https://doi.org/10.1002/adma.19890010312>

46. An, Y., Jiang, G., Qi, Y., et al. “Nano-fluid loss agent based on an acrylamide-based copolymer grafted on a modified silica surface”, *Rsc Advances*, **6**(21), pp. 17246-17255 (2016).
<https://doi.org/10.1039/C5RA24686E>

47. Yongzhong, J., Kun, Z., Yong, Y., et al. “Application of preventing circulation loss and plugging technology of the tiny foam drilling fluid in well Yuhuang 1”, *Drilling & Production Technology*, **28**(3), pp. 95-97 (2005).
<https://doi.org/10.1088/1755-1315/861/7/072034>

48. Xiaojun, W. “The development and application of solid-free micro-foam drilling fluid with temperature resistance and salt tolerance”, *Petroleum Drilling Techniques*, **44**(2), pp. 58-64 (2016).
<https://dx.doi.org/10.11911/syztjs.201602010>

49. Haizhong, Z., Wei, Z., Chun, N., et al. “Application of microbubble drilling fluid technology in Zhongke gas field”, *Western Prospecting Project*, **10**, pp. 39-41 (2018).
<https://doi.org/10.4236/ns.2012.47059>

50. Tengfei, M., Yu, Z., Zhiyong, L., et al. “Evaluation and field application of new microfoam drilling fluid with low-damage and high-performance”, *Oilfield Chemistry*, **38**(4), pp. 571-579 (2021).

51. Yaoyuan, Z., Shuangzheng, M., Jinding, C., et al. “Preparation and performance of a high temperature modified starch filter loss reducer”, *Drilling Fluid & Completion Fluid*, **36**(6), pp. 694-699 (2019).
<https://doi.org/10.3969/j.issn.1001-5620.2019.06.006>

52. Ninghui, D., Zhiyuan, W., and Dianchen, L. “Study on drilling fluid system optimization for preventing collapse in complex formation”, *Drilling and Production Technology*, **43**(6), pp. 103-107 (2020).

53. Tianxiang, Z., Fu, L., Bing, L., et al. “Study on the technology of coalbed methane drilling fluid in the Urumqi mining area of Junggar coalfield”, *Energy Chemical Industry*, **42**(4), pp. 44-49 (2021).
<https://doi.org/10.3787/j.issn.1000-0976.2024.10.015>

Biographies

Wenxi Zhu graduated from China University of Geosciences (Beijing), currently is a lecturer at the School of Civil Engineering and Architecture, Henan University, dedicated to the research of environmentally friendly CGA drilling fluid technology and geothermal cementing system suitable for high-temperature geothermal wells.

Bingjie Wang is master student majoring in Civil Engineering at Henan University. The current research direction is the development of geothermal cementing with high thermal conductivity.

Xiuhua Zheng is working at China University of Geosciences (Beijing), has been engaged in the exploration and development of geothermal resources for a long time. The main research directions include geothermal cementing, high-temperature drilling fluid, and air down-hole hammer drilling technology.